A Cryptic Sulfur Cycle in Oxygen-Minimum–Zone Waters off the Chilean Coast

Don E. Canfield, *et al.*

Science **330**, 1375 (2010);
DOI: 10.1126/science.1196889

A Cryptic Sulfur Cycle in Oxygen-Minimum–Zone Waters off the Chilean Coast

Don E. Canfield,[1]* Frank J. Stewart,[2] Bo Thamdrup,[1] Loreto De Brabandere,[1] Tage Dalsgaard,[3] Edward F. Delong,[2] Niels Peter Revsbech,[4] Osvaldo Ulloa[5]

Nitrogen cycling is normally thought to dominate the biogeochemistry and microbial ecology of oxygen-minimum zones in marine environments. Through a combination of molecular techniques and process rate measurements, we showed that both sulfate reduction and sulfide oxidation contribute to energy flux and elemental cycling in oxygen-free waters off the coast of northern Chile. These processes may have been overlooked because in nature, the sulfide produced by sulfate reduction immediately oxidizes back to sulfate. This cryptic sulfur cycle is linked to anammox and other nitrogen cycling processes, suggesting that it may influence biogeochemical cycling in the global ocean.

Oxygen-minimum zones (OMZs) persist in midwater depths of the global ocean, where large-scale circulation and the sinking and decomposition of surface-derived organics deplete oxygen as compared to higher-surface and deep-water oxygen concentrations (*1*). In some regions such as the eastern tropical Pacific, the Arabian Sea, and the Benguela Current upwelling system, water column oxygen concentrations fall below detection (*2*–*4*), prompting the development of a dynamic nitrogen cycle. In these zones, nitrate is actively reduced to nitrite (*5*, *6*). Nitrite is further converted to N_2 gas through "classic" heterotrophic denitrification (*7*) and the autotrophic anammox process (*8*, *9*) or to NH_4^+ through dissimilative nitrate reduction to ammonium. OMZs account for 33% or more of the loss of fixed nitrogen from the oceans (*10*, *11*), and overall, the nitrogen cycle has been thought to dominate the geochemistry and microbial ecology of these regions.

The recent identification of uncultured *Gammaproteobacteria*, closely affiliated with sulfur-oxidizing symbionts, in OMZ waters off the Chilean coast (*12*) suggests that sulfur cycling may also play an important role in oxygen-free nitrate-rich OMZs. A similar microbial community with a full complement of sulfide-oxidizing and nitrate-reducing genes was found in sulfide-free but nitrate-rich portions of the sulfidic Saanich Inlet (*13*), and a sulfate reducer has been isolated from OMZ waters off the coast of Peru (*14*). Direct evidence for large-scale active sulfur cycling in OMZs, however, is lacking. When sulfide, the product of sulfate reduction, is observed in OMZs, it originates in rare pockets of nitrate and nitrite-depleted water (*15*) or is released from sediments (*6*).

We explored the dynamics of the sulfur cycle in the upwelling waters off Iquique, on the northern Chilean coast, using a combination of geochemical and metagenomic techniques (*16*). In general, the OMZ is well developed in this region of Chile (*17*). We concentrated our efforts on station 3 (20°5′9.27″S, 70°20′8.18″W; water depth 1050 m, 23 km from shore), which, based on preliminary survey data, was in the most biologically active region of the OMZ in our study area. We expanded our geochemical studies to include station 5 (20°5′9.69″S, 70°46′5.78″W; water depth 1500 m), located some 44 km further

[1]Institute of Biology and Nordic Center for Earth Evolution, University of Southern Denmark, Campusvej 55, 5230 Odense M, Denmark. [2]Department of Biological Engineering and Department of Civil and Environmental Engineering, Massachusetts Institute of Technology, Cambridge, MA 02138, USA. [3]National Environmental Research Institute, Aarhus University, Vejlsøvej 25, Post Office Box 314, DK-8600 Silkeborg, Denmark. [4]Section of Microbiology, Department of Biological Sciences, Aarhus University, DK-8000 Aarhus C, Denmark. [5]Departamento de Oceanografía and Centro de Investigación Oceanográfica en el Pacífico Sur-Oriental, Universidad de Concepción, Casilla-160-C, Concepción, Chile.

*To whom correspondence should be addressed. E-mail: dec@biology.sdu.dk

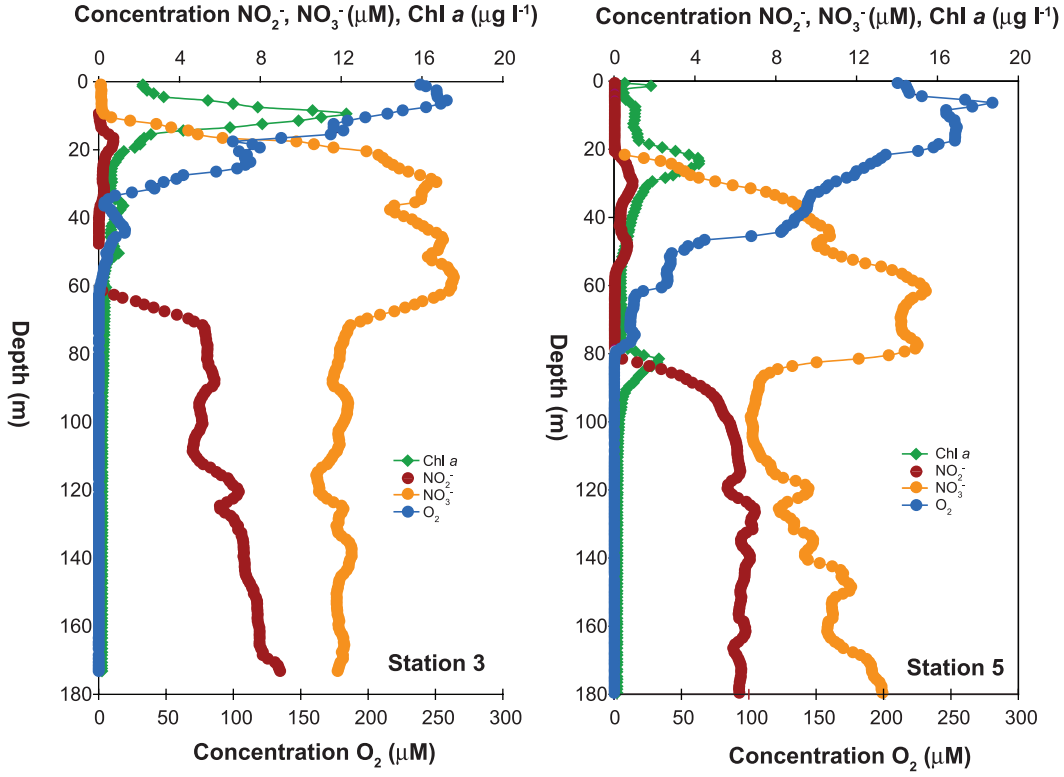

Fig. 1. Representative nutrient, oxygen, and chlorophyll a profiles from the OMZ off the northern Chilean coast at station 3 (**left**) and station 5 (**right**).

offshore than station 3. The water chemistry in the northern Chilean OMZ develops within an eastern boundary current, and the chemical profiles are somewhat dynamic (Fig. 1). With some variability over time, the redoxcline at station 5 was located deeper than at station 3, and although the surface concentrations of chlorophyll a were higher at station 3, we frequently observed a pronounced secondary chlorophyll a maximum at station 5. This deep layer consists of previously unknown members of the cyanobacterial genus *Prochlorococcus* (*18*).

We observed extremely low O_2 concentrations of <13 nM, starting from between 60 and 85 m depth (depending on station and time of sampling) and continuing to >180 m (fig. S1). Similar low values were found off the southern Peruvian coast in an earlier study (*19*), suggesting that essentially anoxic waters define this region of the eastern tropical South Pacific OMZ. There is an upper nitrite maximum related to aerobic processes, but nitrite accumulated as oxygen disappeared in the anoxic core of the OMZ. Nitrate reduction was the most likely source for this nitrite. We measured with ^{15}N-enriched nitrite the rates and pathways of N_2 formation, and similar to what was found in an early study (*8*), anammox was the dominant pathway (Table 1), considerably outpacing denitrification (*16*). The overall rates of N_2 formation were similar to those in previous measurements in this region (*8*).

Table 1. Summary of process rate averages.

	Station 3	Station 5
Process rates (nmol liter^{-1} hour^{-1})		
Anammox	0.43 ± 0.21†	0.29 ± 0.10‡
Denitrification*	0.079 ± 0.04†	0.042 ± 0.029‡
Sulfate reduction	0.51 ± 0.21§	0.055 ± 0.023‖
Depth-integrated rates (mmol m^{-2} day^{-1})		
Anammox	1.21 ± 0.45	0.70 ± 0.24
Denitrification	0.22 ± 0.11	0.10 ± 0.069
Sulfate reduction	1.00 ± 0.40¶	0.28 ± 0.12
Carbon oxidation in OMZ #	5.50	5.50

*Measured as nitrite reduction to N_2. †From 65 to 183 m depth (n = 17). ‡From 73.5 to 173 m depth (n = 16). §From 85 to 150 m depth (n = 8). ‖From 85 to 300 m depth (n = 14). ¶Assuming that sulfate reduction stops first at 200 m. #Estimated from data in (*17*).

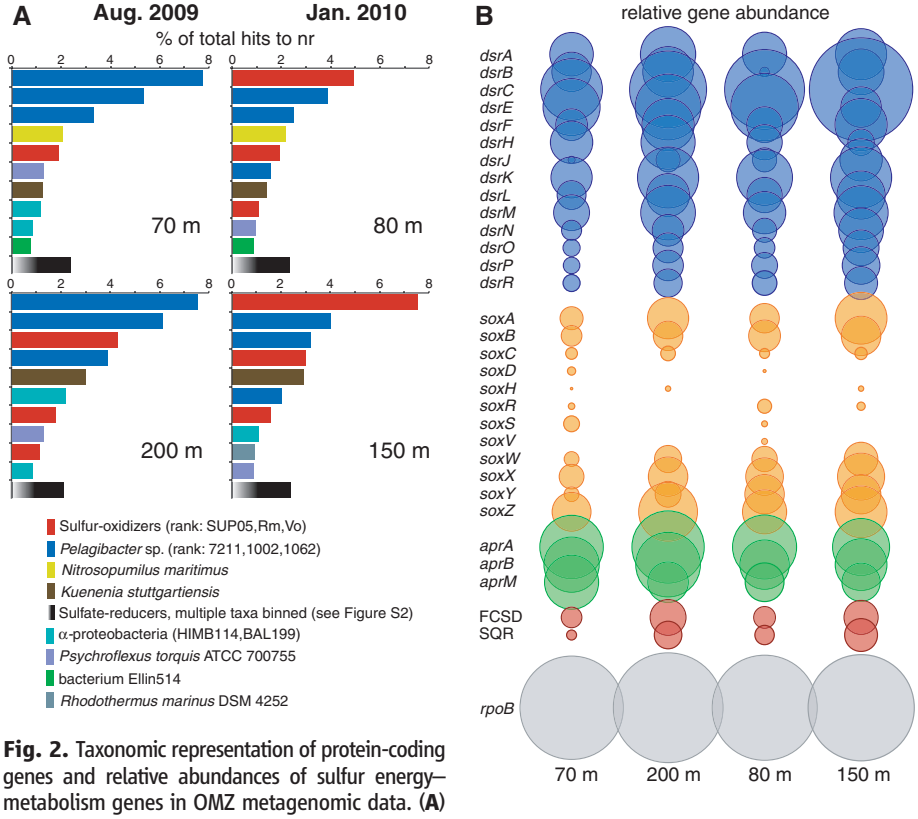

Fig. 2. Taxonomic representation of protein-coding genes and relative abundances of sulfur energy–metabolism genes in OMZ metagenomic data. (**A**) Most abundant taxa identified from annotations of protein-coding genes (in the NCBI-nr database) in pyrosequencing reads from genomic DNA. Reads matching multiple putative sulfate-reducer reference taxa (fig. S1 and table S2) are binned in a single category (black bar). (**B**) Abundances (hit counts per gene) of dissimilatory sulfur metabolism genes, shown relative to the putative single copy per organism of RNA polymerase subunit B (*rpoB*). Abundances per gene are normalized to gene length but not to copy number variation. *dsr*, dissimilatory sulfite reductase gene cluster; *sox*, sulfur oxidation gene cluster; *aprBA*, adenosine 5′-phosphosulfate (APS) reductase; *aprM*, APS reductase membrane anchor; FCSD, flavocytochrome c sulfide dehydrogenase; SQR, sulfide-quinone reductase.

Pyrosequencing of community DNA from below the oxycline (70 to 80 m) and in the core of the anoxic zone (150 to 200 m) at station 3 suggested a substantial role for sulfur-based metabolic pathways in the Chilean OMZ (Fig. 2 and figs. S4 to S7). Gene sequences matching diverse sulfide-oxidizing and sulfate-reducing taxa (table S3) constituted 6.3 to 16.2% and 2.1 to 2.4% of all sequencing reads with matches to protein-coding genes in the National Center for Biotechnology Information–nr (NCBI-nr) database, consistent with percentages based on 16*S* ribosomal RNA gene-encoding reads (figs. S4 and S5). In contrast, sulfur-oxidizer and sulfate-reducer sequences represented only 0.5 and 0.3% of the total protein-coding sequences recovered in an aerobic community from another coastal site (Monterey Bay, 10 m; fig. S5). The Chilean OMZ metagenomes were particularly enriched in sequences matching the genomes of sulfur-oxidizing endosymbionts of deep-sea clams [*Candidatus* Ruthia magnifica (Rm) and *Candidatus* Vesicomyosocius

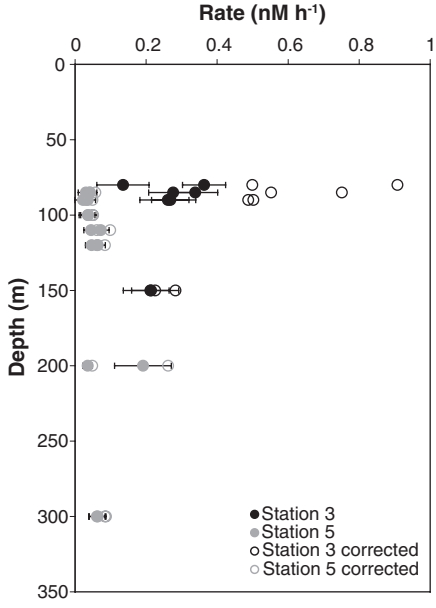

Fig. 3. Sulfide-oxidation corrected and uncorrected rates of sulfate reduction at stations 3 and 5. Standard deviations represent variability during scintillation counting (*16*).

okutanii (Vo) (*20*, *21*)] and the endosymbiont-related SUP05 pelagic lineage from Saanich Inlet (*13*) (Fig. 2A). These taxa increased in abundance in January 2010 (austral summer) relative to samples collected from the same site in August 2009 (late winter). In the January 2010 samples, SUP05-like sequences dominated the identifiable protein-coding gene pool (up to 7.5% of all hits on NCBI-nr). The SUP05 metagenome (*13*) was represented at high coverage, matching 80% of all SUP05 genes (1169 of 1456) with relatively uniform abundances and an average amino acid similarity of 70% (fig. S7). The sulfate-reducing population contributed to a lower but appreciable proportion of sequencing reads and was represented by a diverse population that included *Desulfatibacillum*, *Desulfobacterium*, *Desulfococcus*, *Syntrophobacter*, and *Desulfovibrio* species (figs. S4 to S6).

The prevalence of sulfur-metabolizing taxa was paralleled by a strong representation of sulfur energy–metabolism genes. These genes occur in various combinations across diverse sulfur-utilizing taxa (*22*). Here, genes of the dissimilatory sulfite reductase enzyme (*dsr*), the sulfur oxidation (*sox*) gene complex mediating thiosulfate oxidation, and the adenosine 5′-phosphosulfate (APS) reductase (*apr*) were present throughout the OMZ (Fig. 2B). Several of the proteins encoded by these genes, including *dsr* and *apr* enzymes, function in both oxidative and reductive pathways (*23*, *24*). Here, the majority of the sequences recovered in the OMZ matched known sulfide oxidizers, which is consistent with the high abundance of the SUP05 group. Putative sulfide-oxidizing and sulfate-reducing taxa constituted 62.0 and 2.2% of top hits to *aprA* sequences, respectively, with the remainder matching *aprA* genes of the alphaproteobacterial genus *Pelagibacter*, whose function in sulfide oxidation is not yet clear (*25*) (fig. S6). Overall, the metagenomic data suggest a prevalent summer OMZ community of both oxidative and reductive sulfur-cycling bacteria.

Although our metagenomic libraries suggest an active sulfur cycle, it is cryptic, with no obvious in situ chemical expression. To explore the geochemical importance of the sulfur cycle and possible links to nitrogen cycling, we measured rates of sulfate reduction with $^{35}SO_4^{2-}$ (*26*). We subdued the immediate reoxidation of sulfide produced during sulfate reduction by adding 10 to 13 μM unlabeled sulfide to trap any radiolabeled sulfide from sulfate reduction (*16*). Radiolabeled sulfate was added within 10 hours of sample collection. In some cases, our added unlabeled sulfide was substantially oxidized during the incubations (*16*), implying that radiolabeled sulfide must also have been oxidized and lost as a result. After estimating the loss of radiolabeled sulfide due to sulfide oxidation, we corrected the rates to obtain estimates of the gross sulfate reduction rates (*16*) (Fig. 3). Our findings contrast with the current consensus that sulfate reduction in OMZs will be active only when other more thermodynamically favorable electron acceptors, such as nitrate and nitrite, are fully utilized (*27*). Although not the most favorable, our calculations show that sulfate reduction is still a thermodynamically favorable process in these OMZ waters (*16*). Previous observations of pure cultures of sulfate-reducing bacteria that actively reduce sulfate in the presence of nitrate (*28*, *29*) also support our observations of active sulfate reduction.

Rates of sulfate reduction were much higher at station 3 than at station 5. Indeed, corrected rates at station 3 match and even exceed rates of denitrification and anammox (Table 1), implying that sulfate reduction is an important pathway of organic carbon mineralization at this site. Depth-integrated corrected rates of sulfate reduction at station 3 are equivalent to about 2 mmol of C oxidized m^{-2} day^{-1}, assuming 2 mol of organic carbon oxidized per mole of sulfate reduced. Sediment trap studies at coastal and offshore stations about 200 km south of our study site (*17*) reveal about 5.50 mmol m^{-2} day^{-1} of carbon mineralization within the OMZ waters from between 65 and 300 m depth. If these rates apply to station 3, then sulfate reduction would account for about 33% of the total organic carbon mineralization in the OMZ waters.

Sulfate reduction may also contribute to the ammonium requirements of other indigenous bacteria participating in the anammox process. Indeed, the source of ammonium for anammox has proven elusive because insufficient ammonium is liberated during organic matter decomposition by denitrification to drive measured anammox rates in many OMZ waters (*8*, *9*). In a partial resolution to this dilemma, the dissimilatory reduction of nitrate to ammonium and the heterotrophic reduction of nitrate to nitrite have been identified as significant ammonium sources in OMZ waters off the Peruvian coast (*9*) (the latter due to the ammonium liberated during mineralization of organic matter). But even these extra sources do not account for all of the ammonium demand. From our sulfate reduction rates at station 3, sulfate reduction produces a total of about 0.30 mmol m^{-2} day^{-1}, assuming a 6.6/1 ratio between carbon oxidation and ammonium liberation (*30*). This would contribute 22% of the ammonium needs for anammox at station 3 (Table 1). At station 5, sulfate reduction would contribute only about 8% of the ammonium needs for anammox, underlining the complexity of the nitrogen cycle and the variability of ammonium sources for anammox (*9*).

We also explored the dynamics of sulfide oxidation in these waters and the relationship between sulfide oxidation and the nitrogen cycle (*16*). In parallel with our sulfate reduction rate determinations, we incubated OMZ water from two depths at both stations 3 and 5 with and without added sulfide. Sulfide oxidation was strongly coupled to nitrate reduction to nitrite, and at station 5, nitrate reduction to nitrous oxide was also enhanced with sulfide addition (fig. S8). At station 3, N_2 production from both nitrite and nitrate (at 75 m depth) increased, and in general, rates of sulfide oxidation and subsequent rates of nitrogen turnover were much higher at station 3 than at station 5. This is consistent with the higher rates of sulfate reduction at station 3 and a more active sulfur cycle.

Admittedly, our added levels of sulfide and subsequent rates of sulfide oxidation exceed in situ levels. Nevertheless, our results demonstrate the inherent capacity for active in situ coupling between the sulfur and nitrogen cycles in OMZ zones of the marine water column. This cycling is analogous to that observed at the sulfide/nitrate interface in other strongly redox stratified marine systems (*13*, *31*, *32*) and demonstrates that nitrite, N_2, and N_2O may all be products of this coupling. We speculate that other nitrate-rich oxygen-free OMZs may also house actively coupled sulfur and nitrogen cycles.

References and Notes

1. K. Wyrtki, *Deep-Sea Res.* **9**, 11 (1962).
2. J. D. Cline, F. A. Richards, *Limnol. Oceanogr.* **17**, 885 (1972).
3. D. B. Olson, G. L. Hitchcock, R. A. Fine, B. A. Warren, *Deep Sea Res. Part II Top. Stud. Oceanogr.* **40**, 673 (1993).
4. S. E. Calvert, N. B. Price, *Deep-Sea Res.* **18**, 505 (1971).
5. J. M. Morrison *et al.*, *Deep Sea Res. Part II Top. Stud. Oceanogr.* **46**, 1903 (1999).
6. V. Brüchert *et al.*, *Geochim. Cosmochim. Acta* **67**, 4505 (2003).
7. S. E. Bulow, J. J. Rich, H. S. Naik, A. K. Pratihary, B. B. Ward, *Deep Sea Res. Part I Oceanogr. Res. Pap.* **57**, 384 (2010).
8. B. Thamdrup *et al.*, *Limnol. Oceanogr.* **51**, 2145 (2006).
9. P. Lam *et al.*, *Proc. Natl. Acad. Sci. U.S.A.* **106**, 4752 (2009).
10. L. A. Codispoti *et al.*, *Sci. Mar.* **65**, 85 (2001).
11. J. N. Galloway *et al.*, *Biogeochemistry* **70**, 153 (2004).
12. H. Stevens, O. Ulloa, *Environ. Microbiol.* **10**, 1244 (2008).
13. D. A. Walsh *et al.*, *Science* **326**, 578 (2009).
14. K. W. Finster, K. U. Kjeldsen, *Antonie van Leeuwenhoek* **97**, 221 (2010).
15. R. C. Dugdale, J. J. Goering, R. T. Barber, R. L. Smith, T. T. Packard, *Deep-Sea Res.* **24**, 601 (1977).
16. See supporting material on *Science* Online.
17. R. Escribano *et al.*, *Deep Sea Res. Part II Top. Stud. Oceanogr.* **51**, 2389 (2004).
18. P. Lavin, B. González, J. F. Santibáñez, D. J. Scanlan, O. Ulloa, *Environ. Microbiol. Rep.* 10.1111/j.1758-2229.2010.00167.x (2010).
19. N. P. Revsbech *et al.*, *Limnol. Oceanogr. Methods* **7**, 371 (2009).
20. I. L. G. Newton *et al.*, *Science* **315**, 998 (2007).
21. H. Kuwahara *et al.*, *Curr. Biol.* **17**, 881 (2007).
22. C. Dahl, C. G. Friedrich, Eds., *Microbial Sulfur Metabolism* (Springer-Verlag, Heidelberg, 2008).
23. B. Meyer, J. Kuever, *Microbiology* **153**, 3478 (2007).
24. B. Meyer, J. Kuever, *Microbiology* **153**, 2026 (2007).
25. B. Meyer, J. Kuever, *Appl. Environ. Microbiol.* **73**, 7664 (2007).
26. D. B. Albert, C. Taylor, C. S. Martens, *Deep-Sea Res.* **42**, 1239 (1995).
27. P. N. Froelich *et al.*, *Geochim. Cosmochim. Acta* **43**, 1075 (1979).

28. T. Dalsgaard, F. Bak, *Appl. Environ. Microbiol.* **60**, 291 (1994).
29. R. G. L. McCready, W. D. Gould, F. D. Cook, *Arch. Microbiol.* **135**, 182 (1983).
30. A. C. Redfield, B. H. Ketchum, F. A. Richards, in *The Sea*, N. M. Hill, Ed. (Academic Press, London, 1963), vol. 2, pp. 26–77.
31. M. M. Jensen, J. Petersen, T. Dalsgaard, B. Thamdrup, *Mar. Chem.* **113**, 102 (2009).
32. G. Lavik *et al.*, *Nature* **457**, 581 (2009).

33. We thank the captain and crew of the *Agor Vidal Gormaz* from the Chilean Navy for their kind support, and the Agouron Institute, the Danish National Research Foundation, the Gordon and Betty Moore Foundation, and the Chilean Fondap Program for financial support. Additional thanks to G. Alarcón, G. Friederich, and J. Jennings for operational and experimental support. The genome sequence data are accessible on NCBI's Sequence Read Archive via accession number SRA025088.

Supporting Online Material
www.sciencemag.org/cgi/content/full/science.1196889/DC1
Materials and Methods
Figs. S1 to S8
Tables S1 to S4
References

24 August 2010; accepted 28 October 2010
Published online 11 November 2010;
10.1126/science.1196889

Dynamical Response of the Tropical Pacific Ocean to Solar Forcing During the Early Holocene

Thomas M. Marchitto,[1]* Raimund Muscheler,[2] Joseph D. Ortiz,[3] Jose D. Carriquiry,[4] Alexander van Geen[5]

We present a high-resolution magnesium/calcium proxy record of Holocene sea surface temperature (SST) from off the west coast of Baja California Sur, Mexico, a region where interannual SST variability is dominated today by the influence of the El Niño–Southern Oscillation (ENSO). Temperatures were lowest during the early to middle Holocene, consistent with documented eastern equatorial Pacific cooling and numerical model simulations of orbital forcing into a La Niña–like state at that time. The early Holocene SSTs were also characterized by millennial-scale fluctuations that correlate with cosmogenic nuclide proxies of solar variability, with inferred solar minima corresponding to El Niño–like (warm) conditions, in apparent agreement with the theoretical "ocean dynamical thermostat" response of ENSO to exogenous radiative forcing.

The influence of solar variability on Earth's climate over centennial to millennial time scales is the subject of considerable debate. The change in total solar irradiance over recent 11-year sunspot cycles amounts to <0.1%, but greater changes at ultraviolet wavelengths (*1*) may have substantial impacts on stratospheric ozone concentrations, thereby altering both stratospheric and tropospheric circulation patterns (*2*). Estimates of the secular increase in total irradiance since the late 17th century Maunder sunspot minimum range from ~0.05 to 0.5% (*1*). Values in the middle of this range are sufficient to force the intermediate-complexity Zebiak-Cane model of El Niño–Southern Oscillation (ENSO) dynamics into a more El Niño–like state during the Little Ice Age (A.D. ~1400 to 1850) (*3*), a response dubbed the "ocean dynamical thermostat" because negative (or positive) radiative forcing results in dynamical ocean warming (or cooling, respectively) of the eastern tropical Pacific (ETP) (*4*). This model prediction is supported by paleoclimatic proxy reconstructions over the past millennium (*3*, *5*, *6*). In contrast, fully coupled general circulation models (GCMs) lack a robust thermostat response because of an opposing tendency for the atmospheric circulation itself to strengthen under reduced radiative forcing (*7*).

ENSO is a leading source of interannual climate variability over large regions of the globe, so it is crucial to gain an improved understanding of its past responses to external forcing at various time scales. Tropical fossil corals provide the most reliable means for reconstructing ENSO conditions from the past (*5*), but the record is currently too fragmented to test for any relation to persistent solar forcing before the past millennium. Few sea surface temperature (SST) reconstructions from well-placed tropical Pacific sediment cores have sufficient temporal resolution to address this question.

Sediment core composite MV99-GC41/PC14 was raised from a water depth of 540 m on the floor of Soledad Basin, which is located off the west coast of Baja California Sur, Mexico (25.2°N, 112.7°W), and has an effective sill depth of 290 m (*8*). Although this site is just outside of the tropical band, modern conditions here are strongly teleconnected to ENSO. The modern annual cycle of SST has an amplitude of ~8°C on average, with minimum temperatures during spring, the season of strongest coastal upwelling (*9*, *10*). Yet interannual variability in SST is much more strongly dependent on ENSO than on local upwelling winds. Over the 30-year period covered by satellite observations, the Niño 3 index explains 37% of the monthly SST anomaly near Soledad Basin (correlation coefficient $r = 0.61$ maximum correlation with a 2-month lag), whereas the local upwelling index explains only 2% ($r = -0.16$ with zero lag) (Fig. 1). ENSO is crucial for SST because the regional thermocline deepens during El Niño years, so that even with vigorous local upwelling the ascending waters are warmer than during La Niña or neutral years (*11*). Recent spring SST minima have ranged from 17°C during strong La Niñas to 20°C during

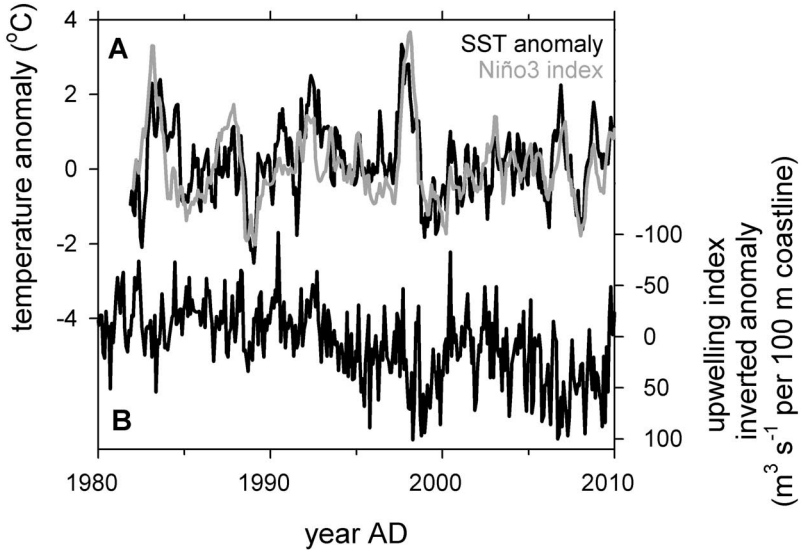

Fig. 1. (**A**) Monthly SST anomaly for the 1° grid cell situated over Soledad Basin (black) (*9*), compared to the monthly Niño 3 SST index on the same vertical scale but lagged by 2 months (gray) (*9*) and (**B**) the local (24°N, 113°W) monthly upwelling index (offshore Ekman transport computed from wind stress) anomaly (*10*), shown inverted.

[1]Department of Geological Sciences and Institute of Arctic and Alpine Research, University of Colorado, Boulder, CO 80309, USA. [2]Department of Earth and Ecosystem Sciences, Lund University, S-223 62 Lund, Sweden. [3]Department of Geology, Kent State University, Kent, OH 44242, USA. [4]Department of Environmental Geosciences, Universidad Autónoma de Baja California, Ensenada, Baja California 22830, Mexico. [5]Lamont-Doherty Earth Observatory, Columbia University, Palisades, NY 10964, USA.

*To whom correspondence should be addressed. E-mail: tom.marchitto@colorado.edu